

ZORRO: Valid, Sparse, and Stable Explanations in Graph Neural Networks

Thorben Funke
funke@l3s.de
L3S Research Center
Hannover, Germany

Megha Khosla
khosla@l3s.de
L3S Research Center
Hannover, Germany

Avishek Anand
anand@l3s.de
L3S Research Center
Hannover, Germany

ABSTRACT

With the ever-increasing popularity and applications of graph neural networks, several proposals have been made to interpret and understand the decisions of a GNN model. Explanations for a GNN model differ in principle from other input settings. It is important to attribute the decision to input features and other related instances connected by the graph structure. We find that the previous explanation generation approaches that maximize the mutual information between the label distribution produced by the GNN model and the explanation to be restrictive. Specifically, existing approaches do not enforce explanations to be predictive, sparse, or robust to input perturbations.

In this paper, we lay down some of the fundamental principles that an explanation method for GNNs should follow and introduce a metric *fidelity* as a measure of the explanation’s effectiveness. We propose a novel approach Zorro based on the principles from *rate-distortion theory* that uses a simple combinatorial procedure to optimize for fidelity. Extensive experiments on real and synthetic datasets reveal that Zorro produces sparser, stable, and more faithful explanations than existing GNN explanation approaches.

ACM Reference Format:

Thorben Funke, Megha Khosla, and Avishek Anand. 2018. ZORRO: Valid, Sparse, and Stable Explanations in Graph Neural Networks. In *Woodstock ’18: ACM Symposium on Neural Gaze Detection, June 03–05, 2018, Woodstock, NY*. ACM, New York, NY, USA, 12 pages. <https://doi.org/10.1145/1122445.1122456>

1 INTRODUCTION

Graph neural networks (GNNs) are a flexible and powerful family of models that build representations of nodes or edges on irregular graph-structured data and have experienced significant attention in recent years. These methods are based on the so-called “neighborhood aggregation” scheme. A node representation is learned by aggregating features from their neighbors, and GNNs have achieved state-of-the-art performance on node and graph classification tasks. We focus on explaining or interpreting the rationale underlying a given prediction of already trained GNNs for node classification.

We aim to explain the decision of an already trained GNN model (post-hoc interpretability) by attributing the reason for the underlying decision to either a subset of features or neighboring nodes, or both. Current approaches to explain GNNs [21, 26, 31] produce feature attributions in a post-hoc manner, but they suffer from some fundamental limitations.

Firstly, existing explanation approaches output distributions or soft-masks over input features or nodes [31]. However, humans find it hard to make sense of soft-masks and instead prefer sparse binary masks or hard-masks [1, 13, 18]. Secondly, existing explanation methods, like gradient-based feature attribution techniques [24], might not be predictive. Finally, current explainability approaches do not optimize for stability in input perturbations. Existing approaches do not have such explicit stability objectives and hence are usually not stable.

To systematically fill in the above gaps, we commence by formulating three desired properties of a GNN explanation: *sparsity*, *validity*, and *stability*. Figure 1 provides an illustration of the three properties.

Validity. *We say that an explanation is valid if the model’s label is predictable alone from the input nodes and features selected by the explanation.*

It is easy to see that validity alone is not sufficient for an explanation as the full input is a valid explanation [27]. Ideally, the explanation should only highlight parts of the input with the highest predictive power. In addition to being more human-understandable, a short explanation is more comfortable to analyze for any downstream applications for explanations [10].

Sparsity. *The smaller the explanation size, the sparser is the explanation.*

We argue that validity and sparsity, though necessary, are not sufficient to define an explanation. In Section 2.2, we show that the trivial empty explanation (all features are replaced by 0s) could be a valid explanation for many cases. The high validity observed in such cases is an artifact of a particular configuration of trained model parameters. Moreover, the effect is exaggerated in GNNs in which the complex dependencies among the nodes (instances) of the graph is encoded in the model itself.

We would expect that the model retains its predictive power with only the knowledge of the explanation *while the rest of the information in the input is filled randomly*. In other words, an explanation should be valid independent of the rest of the input.

Stability. *An explanation is stable if it stays valid for different configurations of other parts of the input (not part of the explanation).*

In this paper, we introduce a new metric called *fidelity* which is grounded in the principles of *rate-distortion theory* and reflects

Permission to make digital or hard copies of all or part of this work for personal or classroom use is granted without fee provided that copies are not made or distributed for profit or commercial advantage and that copies bear this notice and the full citation on the first page. Copyrights for components of this work owned by others than ACM must be honored. Abstracting with credit is permitted. To copy otherwise, or republish, to post on servers or to redistribute to lists, requires prior specific permission and/or a fee. Request permissions from permissions@acm.org.

Woodstock ’18, June 03–05, 2018, Woodstock, NY

© 2018 Association for Computing Machinery.

ACM ISBN 978-1-4503-XXXX-X/18/06...\$15.00

<https://doi.org/10.1145/1122445.1122456>

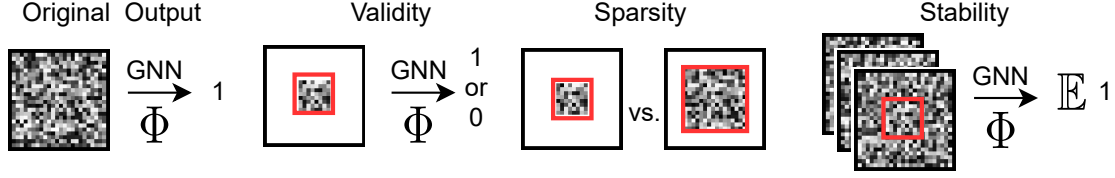


Figure 1: Illustration of validity, sparsity, and stability. The GNN Φ takes the feature matrix X , which is illustrated as a grayscale matrix, and the relations from the graph G , which is not shown for simplicity, to predict the class label (1). An explanation selects the most important inputs from the feature matrix responsible for the prediction, which we illustrate as red rectangles. The validity of an explanation is the property to preserve the prediction if a fixed baseline value replaces all not selected values. The sparsity is the number of selected elements, where fewer elements are desirable. Lastly, stability is the property to preserve the prediction if all not selected values are perturbed. Existing methods only optimize for validity and sparsity. However, even trivial explanations can be valid and sparse. We introduce *fidelity* as the new measure which also accounts for explanation stability and present ZORRO to retrieve valid, sparse, and stable explanations.

these three desiderata into a single measure. Essentially, we cast the problem of finding explanations given a trained model as a signal/message reconstruction task involving a sender, a receiver, and a noisy channel. The message sent by the sender is the actual feature vector, with the explanation being a subset of immutable feature values. The noisy channel can obfuscate only the features that do not belong to the explanation. The explanation’s fidelity lies in the degree to which the decoder can faithfully reconstruct from the noisy feature vector. Optimizing fidelity is NP-hard, and we consequently propose a greedy combinatorial procedure ZORRO that generates sparse, predictive, and stable explanations.

Accurately measuring the actual effectiveness of post-hoc explanations has been acknowledged to be a challenging problem due to the lack of explanation ground truth. We carry out an extensive and comprehensive experimental study on several experimental regimes [8, 21, 31], three real-world datasets [30] and four different GNN architectures [14, 15, 25, 29] to evaluate the effectiveness of our explanations. In addition to measuring validity, sparsity, and fidelity, we also compare our approach with respect to the evaluation regime proposed in GNNEXPLAINER, consistency and faithfulness measures proposed in [21] and the ROAR methodology from [8].

Firstly, we establish that ZORRO outperforms all other baselines over different evaluation regimes and datasets. Specifically, it shows an improvement of at least 32.87% up to more than 90% over real-world datasets compared to GNNEXPLAINER. Interestingly, we find that, under our definition of fidelity, explanations from the popular gradient-based explanation methods have only slightly higher fidelity values than a naïve/trivial explanation for simple synthetic datasets. Furthermore, we show that ZORRO can retrieve multiple high fidelity explanations for 50% of the nodes.

Next, we clearly show that our explanations also have utility in model understanding and reflect the model behaviors and dataset characteristics. Specifically, we were able to establish insights about homophily affects the GNN model just from the explanations from ZORRO. To sum up, our main contributions are:

- We theoretically investigate the key properties of *validity*, *sparsity* and *stability* that a GNN explanation should follow.

- We introduce a novel evaluation metric, *fidelity* derived from principles of *rate-distortion theory* that reflects these desiderata into a single measure.
- We propose a simple combinatorial called ZORRO to find high fidelity explanations with theoretically bounded stability. We **release our code** at <https://anonymous.4open.science/r/547179ef-e9b8-471c-9d05-616387d03c4b/>.
- We perform extensive scale experiments on synthetic and real-world datasets. We show that ZORRO not only outperforms baselines for fidelity but also for several evaluation regimes so far proposed in the literature.

2 PROPERTIES OF GNN EXPLANATIONS

2.1 Background on GNNs

Let $G = (V, E)$ be a graph where each node is associated with d -dimensional input feature vector. GNNs compute node representations by recursive aggregation and transformation of feature representations of its neighbors which are finally used for label prediction. Formally for a L -layer GNN, let $\mathbf{x}_n^{(\ell)}$ denote the feature representation of node $n \in V$ at a layer $\ell \in L$ and \mathcal{N}_n denotes the set of its direct neighbors. $\mathbf{x}_n^{(0)}$ corresponds to the input feature vector of n . The ℓ -th layer of a GNN can then be described as an aggregation of node features from the previous layer followed by a transformation operation.

$$\mathbf{z}_n^{(\ell)} = \text{AGGREGATION}^{(\ell)} \left(\left\{ \mathbf{x}_j^{(\ell-1)} \mid j \in \mathcal{N}_n \cup \{n\} \right\} \right) \quad (1)$$

$$\mathbf{x}_n^{(\ell)} = \text{TRANSFORMATION}^{(\ell)} \left(\mathbf{z}_n^{(\ell)} \right) \quad (2)$$

Each GNN defines its aggregation function, which is differentiable and usually a permutation invariant function. The transformation operation is usually a non-linear transformation, such as employing ReLU non-linear activation. The final node’s embedding $\mathbf{z}_n^{(L)}$ is then used to make the predictions

$$\Phi(n) \leftarrow \text{argmax } \sigma(\mathbf{z}_n^{(L)} \mathbf{W}), \quad (3)$$

where σ is a sigmoid or softmax function depending on whether the node belongs to multiple or a single class. \mathbf{W} is a learnable weight

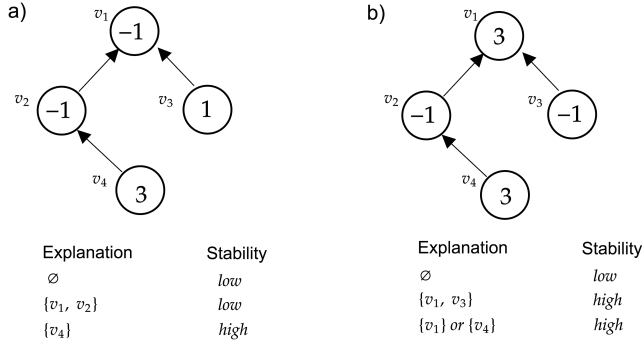


Figure 2: In this synthetic example, we approximate the (node) classification of v_1 by GNN with a rule based on the sum of the node features $\sum f(v_i)$. All given explanations are predictive (when the unselected input is set to 0) and sparse. However, we see that in a) the explanation $\{v_1, v_3\}$ has the same stability as the trivial mask. Example b) highlights that selecting additional elements may not decrease the stability and that even two disjoint explanations are possible.

matrix. The i th element of $z_n^{(L)}\mathbf{W}$ corresponds to the (predicted) probability that node n is assigned to some class i .

2.2 Defining GNN Explanation, Validity and Sparsity

We are interested in explaining the prediction of a GNN $\Phi(n)$ for any node n . We note that for a particular node n the subgraph taking part in the computation of neighborhood aggregation operation, see Eq. (1), fully determines the information used by GNN to predict its class. In particular, for a L -layer GNN, this subgraph would be the graph induced on nodes in the L -hop neighborhood of n . For brevity, we call this subgraph the *computational graph* of the query node. We want to point out that the term "computational graph" should not be confused with the neural network's computational graph.

Let $G(n) \subseteq G$ denote the computational graph of the node n . Let $X(n)$, or briefly X denotes the feature matrix restricted to the nodes of $G(n)$, where each row corresponds to a d -dimensional feature vector of the corresponding node in the computational graph. We define explanation $\mathcal{S} = \{F_s, V_s\}$ as a subset of input features and nodes. In principle \mathcal{S} would correspond to the feature matrix restricted to features in F_s of nodes in V_s . We quantify the validity and sparsity of \mathcal{S} as follows.

Validity. The validity score of explanation \mathcal{S} is 1 if $\Phi(\mathcal{S}) = \Phi(X)$ and 0 otherwise.

In literature validity of an explanation is usually computed with respect to the baseline 0, i.e., we set values of all features not in \mathcal{S} to 0. One can also use feature averages instead of 0.

Sparsity. The sparsity of an explanation is measured as the ratio of bits required to encode an explanation to those required to encode the input. We use explanation entropy to compare sparsity for a fixed input and call this the effective explanation size.

2.3 Limitations of Validity and Sparsity

We illustrate the limitations of previous works, which are based on maximizing validity and sparsity of explanations by a simple example shown in Figure 2. The example is inspired by the example for text analysis by Camburu et al. [3].

The input is a graph with node set $V = \{v_1, v_2, v_3, v_4\}$. Each node has a single feature, with the value given in the Figure. Let us assume that feature values lie in the range from -2 to 3 . For any node v , we define the model output in terms of simple sum (aggregation) of feature values, $f(v)$ of itself and its two hop-neighborhood. For example,

$$\Phi(v_1) = \begin{cases} 1, & \text{if } f(v_1) + f(v_2) + f(v_3) + f(v_4) \geq 0, \\ 0, & \text{otherwise.} \end{cases}$$

Now we wish to explain the prediction $\Phi(v_1) = 1$.

Consider an explanation $\{v_1, v_3\}$. Clearly it is valid explanation with a validity score of 1, if we set the not selected nodes' features to 0. But if we set $f(v_4) = -2, f(v_2) = 0$, the explanation $\{v_1, v_3\}$ is no longer valid.

Similarly, the empty explanation, $\mathcal{S} = \emptyset$, is the sparsest possible explanation which has validity score of 1 when all feature values are set to 0. But for a different realization of the not important features, say for $f(v_2) = -1$ and rest all are set to 0, the validity score is reduced to 0.

We want to emphasize that a particular explanation $\{v_1, v_3\}$ or an empty explanation might be valid for an individual configuration of the features of not selected vertices but not for others. However, a proper explanation should explain the model's prediction independent of the remaining input configuration.

This subtle point is usually ignored by existing interpretability works, which only evaluate an explanation for a specific baseline of the irrelevant part of the input. In contrast, we propose stability, which takes into account the variance of the validity of an explanation over different configurations of the input's unselected parts.

Stability. Let \mathcal{Y} be the distribution of validity for different realizations of $X \setminus \mathcal{S}$. Let $\text{Var}(\mathcal{Y})$ denote the variance of \mathcal{Y} . We define stability $\gamma(\mathcal{S})$ of an explanation, \mathcal{S} as

$$\gamma(\mathcal{S}) = \frac{1}{1 + \text{Var}(\mathcal{Y})}.$$

Note that $\gamma(\mathcal{S}) \in (0, 1]$ and achieves, on the one hand, maximum value of 1 when $\text{Var}(\mathcal{Y}) = 0$, i.e., when the explanation is completely independent of components in $X \setminus \mathcal{S}$. On the other hand, the stability will also be equal to 1 if the validity of an explanation for all realizations is equal to zero. Mathematically, to ensure high predictive power we need to ensure a high expected value of \mathcal{Y} in addition to its low variance. Therefore, we need another metric along with stability, which could also quantify the predictive power of the explanation.

We introduce a novel metric called *fidelity* which quantifies the predictive power as well as the stability of an explanation. Moreover, fidelity has sound theoretical grounding in the area of *rate-distortion theory* [23]. We describe fidelity and its relation to rate-distortion theory and stability in the next section.

3 RATE-DISTORTION THEORY AND FIDELITY

Rate-distortion theory addresses the problem of determining the minimum number of bits per symbol (also referred to as *rate*) that should be communicated over a channel so that the source signal can be approximately reconstructed at the receiver without exceeding an expected distortion, D . The functions relating to rate and distortion are found by optimizing for the following objective.

$$\inf_{Q(S|X)} I_Q(S, X) \text{ such that } \mathbb{E}_Q(D(S, X)) \leq D^*, \quad (4)$$

where $I(S, X)$ denotes the mutual information between input X and compressed signal S , $Q(S|X)$ is the conditional probability density function of the compressed signal S given the input X and D^* corresponds to maximum allowed distortion. Note that Eq. (4) requires minimization of mutual information between X and S . Mutual information will be minimized when S is completely independent of X .

In our explanation framework, the compressed signal S corresponds to an explanation. The effect of minimizing the mutual information between the compressed signal and the input, see Eq. (4), would amount to minimize the size of S . A trivial solution of the empty set is avoided by restricting the average distortion of S in the second part of the objective. In particular, compressed signal (explanation) should be such that knowing only about the input on S and filling in the rest of the information randomly will almost surely preserve the desired output signal (or class prediction).

In particular, for graph models, the explanation S which is a subset of input nodes as well as input features, is most relevant for a classification decision if the expected classifier score remains nearly the same when randomizing the remaining input $X \setminus S$.

More precisely, we formulate the task of explaining the model prediction for a node n , as finding a partition of the components of its computational graph into a subset, S of relevant nodes and features, and its complement S^c of non-relevant components. In particular, the subset S should be such that fixing its value to the true values already determines the model output for almost all possible assignments to the non-relevant subset S^c . The subset S is then returned as an explanation. As it is a rate-distortion framework, we are interested in an explanation (compressed signal) with the maximum agreement (minimum distortion) with the actual model's prediction on complete input. This agreement, what we refer to as *fidelity* is quantified by the expected validity score of an explanation over all possible configurations of the complement set S^c .

3.1 Fidelity

To formally define fidelity, let us denote with Y_S the perturbed feature matrix obtained by fixing the components of the S to their actual values and otherwise noisy entries. The values of components in S^c are then drawn from some noisy distribution, \mathcal{N} . Let $\mathcal{S} = \{V_s, F_s\}$ be the explanation with selected nodes V_s and selected features F_s .

Let $M(S)$, or briefly M , be the mask matrix such that each element $M_{i,j} = 1$ if and only if i th node (in $G(n)$) and j th feature are included in sets V_s and F_s respectively and 0 otherwise. Then the

perturbed input is given by

$$Y_S = X \odot M(S) + Z \odot (\mathbb{1} - M(S)), Z \sim \mathcal{N}, \quad (5)$$

where \odot denotes an element-wise multiplication, and $\mathbb{1}$ a matrix of ones with the corresponding size.

Fidelity. The fidelity of explanation S with respect to the GNN Φ and the noise distribution \mathcal{N} is given by

$$\mathcal{F}(S) = \mathbb{E}_{Y_S|Z \sim \mathcal{N}} [\mathbb{1}_{\Phi(X)=\Phi(Y_S)}]. \quad (6)$$

In simple words, fidelity is computed as the expected validity of the perturbed input Y_S .

Note that high fidelity explanations would be stable by definition, i.e., their validity score would not vary greatly across different realizations of S^c .

THEOREM 1. An explanation with fidelity p has stability value of $\frac{1}{1+p(1-p)}$.

PROOF. Let \mathcal{Y} be the random variable corresponding to validity score for a realization of S^c . Now note that \mathcal{Y} follows a Bernoulli distribution with a mean equal to the expected value of validity, i.e., fidelity. The variance of a Bernoulli distributed variable \mathcal{Y} is given by $p(1-p)$. The proof is completed then by substituting the variance in the definition of stability. \square

Theorem 1 implies that for fidelity greater than 0.5, the stability increases with an increase in fidelity and achieves a maximum value of 1 when fidelity reaches its maximum value of 1. Therefore, to ensure high stability, it suffices to find high fidelity explanations. As stability is theoretically bounded with respect to fidelity, we do not additionally report stability in our experiments.

4 MAXIMIZING EXPLANATION FIDELITY

We propose a simple but effective greedy combinatorial approach, which we call ZORRO, to find high fidelity explanations. By fixing the fidelity to a certain user-defined threshold, say τ , we are then interested in the sparsest explanation, which has a fidelity of at least τ .

The pseudocode is provided in Algorithm 1. Let for any node n , V_n denote the vertices in its computational graph $G(n)$, i.e., the set of vertices in L -hop neighborhood of node n for an L -layer GNN; and F denote the complete set of features. We start with zero-sized explanations and select as first element

$$\operatorname{argmax}_{f \in F} \mathcal{F}(V_n, \{f\}) \quad \text{or} \quad \operatorname{argmax}_{v \in V_n} \mathcal{F}(\{v\}, F), \quad (7)$$

whichever yields the highest fidelity value. We iteratively add new features or nodes to the explanation such that the fidelity is maximized over all evaluated choices. Let V_p and F_p respectively denote the set of possible candidate nodes and features that can be included in an explanation at any iteration. We save for each possible node $v \in V_p$ and feature $f \in F_p$ the ordering R_{V_p} and R_{F_p} given by the fidelity values $\mathcal{F}(\{v\}, F_p)$ and $\mathcal{F}(V_p, \{f\})$ respectively. To reduce the computational cost, we only evaluate each iteration the top K remaining nodes and features determined by R_{V_p} and R_{F_p} .

As shown in Fig. 2, an instance can have multiple valid, sparse, and stable explanations. Therefore, we also propose a variant of ZORRO, which continues searching for further explanations: Once

Algorithm 1 ZORRO(n, τ, K)

```

1:  $V_n \leftarrow$  set of vertices in  $G(n)$ 
2:  $F_p \leftarrow$  set of node features
3:  $V_r = V_p, F_r = F_p, V_s = \emptyset, F_s = \emptyset$ 
4:  $R_{V_p} \leftarrow$  list of  $v \in V_p$  sorted by  $\mathcal{F}(\{v\}, F_p)$ 
5:  $R_{F_p} \leftarrow$  list of  $f \in F_p$  sorted by  $\mathcal{F}(V_p, \{f\})$ 
6: Add maximal element to  $V_s$  or  $F_s$  as in (7)
7: while  $\mathcal{F}(V_s, F_s) \geq \tau$  do
8:    $\tilde{V}_s = V_s \cup \operatorname{argmax}_{v \in \operatorname{top}_K(V_r)} \mathcal{F}(\{v\} \cup V_s, F_s)$ 
9:    $\tilde{F}_s = F_s \cup \operatorname{argmax}_{f \in \operatorname{top}_K(F_r)} \mathcal{F}(V_s, \{f\} \cup F_s)$ 
10:  if  $\mathcal{F}(\tilde{V}_s, \tilde{F}_s) \leq \mathcal{F}(V_s, \tilde{F}_s)$  then
11:     $F_r = F_r \setminus \{f\}, F_s = \tilde{F}_s$ 
12:  else
13:     $V_r = V_r \setminus \{v\}, V_s = \tilde{V}_s$ 
14: return  $\{V_s, F_s\}$ 

```

we found an explanation with the desired fidelity, we discard the chosen elements from the feature matrix X , i.e., we never consider them again as possible choices in computing the next explanation. We repeat the process by finding relevant selections disjoint from the ones already found. To ensure that disjoint elements of the feature matrix X are selected, we recursively call Algorithm 1 with either remaining (not yet selected in any explanation) set of nodes or features. Finally, we return the set of explanations such that the fidelity of τ cannot be reached by using all the remaining components that are not in any explanation. For a detailed explanation of the details and the reasoning behind various design choices, we refer to Appendix A.

The pseudocode to compute fidelity is provided in Algorithm 2. Specifically we generate the obfuscated instance for a given explanation $\mathcal{S} = \{V_s, F_s\}$, $Y_{\mathcal{S}}$ by setting the feature values for selected node-set V_s corresponding to selected features in F_s to their true values. To set the irrelevant values, we randomly choose a value from the set of all possible values for that particular feature in the dataset \mathcal{X} . To approximate the expected value in Eq. (6), we generate a finite number of samples of $Y_{\mathcal{S}}$. We then compute fidelity as average validity with respect to these different baselines.

Algorithm 2 $\mathcal{F}(V_s, F_s)$

```

1: for  $i = 0, \dots, \text{samples}$  do
2:   Set  $Y_{\{V_s, F_s\}}$ , i.e. fix the selected values and otherwise retrieve random values from the respective columns of  $\mathcal{X}$ 
3:   if  $\Phi(Y_{\{V_s, F_s\}})$  matches the original prediction of the model then
4:      $\text{correct} += 1$ 
5: return  $\frac{\text{correct}}{\text{samples}}$ 

```

THEOREM 2. ZORRO has the following properties.

- (1) ZORRO retrieves explanation with at least fidelity τ .
- (2) The runtime of ZORRO is independent of the size of the graph.
The runtime complexity of ZORRO for retrieving an explanation

is given by

$$O(t \cdot \max(|V_n|, |F|))$$

where t is the run time of the forward pass of the GNN Φ .

- (3) ZORRO can retrieve multiple explanations with fidelity at least τ .
- (4) For any retrieved explanation \mathcal{S} and $\tau \geq 0.5$, the stability score is $\gamma(\mathcal{S}) \geq \frac{1}{1+\tau(1-\tau)}$.

For the proof, we refer to appendix B.

5 EXPERIMENTS

Evaluation of post-hoc interpretability techniques has always been tricky owing to the lack of ground truth against which the generated explanations can be compared. Specifically, for a model prediction, collecting the ground truth explanation is akin to asking the trained model what it was thinking about – an impossibility and hence a dilemma. There is no clear solution to the ground-truth dilemma. However, previous research has attempted varying experimental regimes, each with their simplifying assumptions. We conduct a comprehensive set of experiments adopting two existing experimental regimes adopted in the literature – synthetic graphs with ground truth and real graphs without explanation ground truth. We also reflect on the limitations of their assumptions and the threats they might pose to our results’ validity.

5.1 Methods

We choose to compare ZORRO with two widely used baselines, along with a naïve baseline:

GNNEExplainer. Motivated by the optimization of the mutual information between the masked explanation and the original GNN’s prediction, Ying et al. [31] maximize the class probability of the predicted class with edge and feature masks as well as regularization terms. We use their default parameter settings for training and regularization.

Grad & GradInput. In these methods, we take the gradient of the rows and columns of the input feature matrix X , which corresponds to the features’ and nodes’ importance. For GradInput, we also multiply the result element-wise with the input [22].

Empty Explanation. Besides, we evaluate a simple baseline, where the explanation \mathcal{S} is an empty set.

ZORRO. For ZORRO, we retrieved explanations for the thresholds $\tau = .85$ and $\tau = .98$ with $K = 10$. All fidelity values were calculated based on 100 samples. We refer to appendix C and the available implementation for further details of the models and the training of the GNNs.

5.2 Datasets & Evaluation Methodologies

5.2.1 Synthetic Dataset. In GNNEExplainer [31], the authors proposed to use synthetic graph datasets built from attaching motifs, such as houses, grids, or rings, to random Barabási–Albert (BA) graphs or regular trees. The underlying assumption is that: if we construct synthetic graphs with identifiable structures that are “assumed” to be learned by the GNN model, one can check if the explanations identify these structures. We evaluate the synthetic dataset, which has features. As GNN for the synthetic dataset, we

follow Ying et al. [31] and use a three-layer stacked graph convolutional network (GCN) [14].

Accuracy and Precision. The task is to explain all the nodes from the house motif, and the ground truth nodes are the five nodes from the corresponding house. Knowing the “explanation ground truth” in this synthetic setting, we retrieve explanations for the motif nodes and measure the *accuracy* and *precision* of the generated explanation. **Accuracy** is calculated as the fraction of a total number of nodes that are correctly classified as an explanation or not. Clearly, for larger input sizes with short explanations, an empty explanation can also give a high accuracy (also see Table 1). **Precision** is defined as the fraction of returned nodes that are also in the explanation set. Precision provides more reliable results than accuracy when the input is much larger than the explanation. To compute accuracy and precision for baselines, we transform the baselines’ results into a node mask of the five most important nodes, which is the size of the explanation ground truth.

Sparsity and Fidelity. Additionally, we report the *sparsity* and *fidelity* of the explanations. For **sparsity**, we report effective explanation size. In particular, we normalize the node and feature mask returned by the explanation method and then compute the normalized mask’s entropy. As ZORRO returns a binary mask, effective explanation size for ZORRO is given by log of number of selected nodes. **Fidelity** is approximated as average validity over 100 realizations of the perturbed input.

Consistency and Faithfulness. Following Sanchez-Lengeling et al. [21], we also evaluate the explanation methods’ performance for different instances (consistency) of the same GNN and models with different performances (faithfulness). For the first, we repeated the above evaluation for five different GCN, which were trained for different random initializations. The variation in the results is according to [21] an indicator for consistency. For the latter, we recorded the model parameters at different epochs during training and also recorded the performance, see Fig. 6 in appendix C.

5.2.2 Real-World Datasets. We use the datasets **Cora**, **CiteSeer** and **PubMed** [30]. We evaluate our approach on four different two-layer graph neural networks: **GCN**, graph attention network (**GAT**) [25], the approximation of personalized propagation of neural predictions (**APPNP**) [15], and graph isomorphism network (**GIN**) [29]. We evaluate these combinations with respect to *validity*, *sparsity*, and *fidelity* for 300 randomly selected nodes.

Evaluation with ROAR. Furthermore, we follow the remove and retrain (ROAR) approach from Hooker et al. [8]. Following ROAR, we retrain the GNN using $k \in \{1, 5, 10, 50, 100\}$ most important features, returned by the explanation methods, and measure the performance drop with the model’s test accuracy. In detail, we performed the following: We retrieved the explanations for all GCN training nodes on Cora and selected the top k features, which were most often in the explanation. Similarly, we retrieved all the baselines’ explanations and selected the top k features with the highest summed feature mask values. Then we retrain the GCN multiple times on the limited feature set and record the achieved accuracy on the test set.

We also confirm our intuition of Fig. 2 that multiple explanations exist. Therefore, we executed our ZORRO variant, which can

retrieve multiple disjoint explanations, with $\tau = .85$. Finally in Section 5.6, we illustrate the usefulness of ZORRO’s explanations to study differences in models’ behavior.

5.3 Results for Synthetic Dataset

Table 1 shows the performance of ZORRO with $\tau = .85$ and $\tau = .98$, and the baselines. We observe that while the gradient-based methods retrieve the highest recall, ZORRO achieves the best precision, sparsity, stability, and fidelity. More importantly, unlike the baselines ZORRO does not need the prior knowledge of the exact size of the ground truth. For example, for synthetic networks where the ground truth contains five important nodes, ZORRO retrieves explanations with fewer than five nodes, which are already sufficient to explain the GNN’s prediction.

Table 1: Performance of the node explanation on the synthetic dataset. The sparsity is calculated for the retrieved node mask. The high accuracy with empty explanation by large size of negative set. This also points to the pitfall of using Accuracy alone as the measure of evaluating explanations when ground truth is available.

Method	Prec. \uparrow	Accuracy \uparrow	Sparsity \downarrow	Fidelity \uparrow
GNNExplainer	0.40	0.81	1.68	0.63
Grad	0.87	0.95	1.61	0.70
GradInput	0.89	0.96	1.61	0.56
\emptyset - Explanation	0.00	0.84	0.00	0.55
ZORRO ($\tau = .85$)	0.95	0.90	0.65	0.91
ZORRO ($\tau = .98$)	0.90	0.90	1.04	0.98

Table 2 shows the model’s and explainers’ accuracies for the selected epochs. ZORRO achieves the first accuracy peak at 200 epochs, where the model still cannot differentiate the motif from the BA nodes. The gradient-based methods even achieve the best or close to the best performance for the untrained GCN. Hence, for evaluation of node classification explanations, this approach is for this synthetic configuration not suitable. We also analyzed the consistency by repeating the experiments reported in Table 1 five times, but all methods achieved minor variations in the results.

5.4 Results for Real-World Datasets

We report the achieved sparsity, fidelity, and validity of the explanation methods in Table 3. In all evaluation measures, datasets, and models, ZORRO outperforms all other explanation methods. As expected, the explanations of ZORRO for $\tau = 0.85$ are sparser than those for $\tau = 0.98$. In contrast, the ZORRO’s explanation for $\tau = 0.98$ achieve higher fidelity and validity scores than those for $\tau = .85$.

For real-world datasets, the sparsity of GNNEXPLAINER’s explanation is the second-best method and retrieved similar-sized explanations for all GNN models. It also outperforms gradient-based methods and trivial baseline in terms of fidelity. Even if GNNEXPLAINER optimizes implicitly for predictiveness, ZORRO outperforms GNNEXPLAINER in fidelity by at least 36.61% in Cora, 40.57% in Cite-seer and 32.87% for PubMed.

The empty explanation baseline results show that even without selecting any feature value, it achieves validity between 0.11 and

Table 2: Experiments on faithfulness according to Sanchez-Lengeling et al. [21] measured with Kendall’s tau τ_{Kendall} of the retrieved precision. To simulate different model performances, we saved the GCN model during different epochs on the synthetic dataset. For ZORRO $\tau = .85$, the ordering of the explanations’ performances nearly perfectly align with the order of the models performance.

Method	1	200	400	600	1400	2000	τ_{Kendall}
GNNEXPLAINER	0.50	0.54	0.41	0.40	0.37	0.40	−0.73
Grad	0.94	0.80	0.62	0.73	0.84	0.87	0.07
GradInput	0.88	0.89	0.78	0.79	0.87	0.89	0.07
ZORRO ($\tau = .85$)	0.00	0.92	0.88	0.93	0.94	0.94	0.73
ZORRO ($\tau = .98$)	0.00	0.90	0.85	0.84	0.87	0.90	0.47

0.50. Especially for PubMed with only three classes, this heuristic retrieves remarkably average validities, which are often only slightly inferior to the gradient-based methods’ validity. Overall, the gradient-based methods Grad and GradInput perform worse on the real-world datasets.

Since GNNEXPLAINER retrieves edge masks instead of node masks, we compared all approaches based on the effective explanation sizes for the features, i.e., calculated the entropy of the feature masks. For the explained GNN, GIN requires the densest explanation and has for Cora and CiteSeer the lowest validity scores. Fixing the GNN and using ZORRO, the achieved sparsity is the lowest for PubMed and the highest for Cora. Hence, a larger number of possible features does not necessarily correspond to more relevant features.

Our ROAR inspired benchmark confirms the performance of ZORRO. ZORRO outperforms all baselines in all cases. Using only the 10 most important features with respect to ZORRO ($\tau = .98$) already achieves a test accuracy of 0.72 compared to 0.79 on all 1433 features. While selecting 100 features with ZORRO ($\tau = .98$), causes only a minor performance drop of $\Delta < 0.01$. Similarly to Table 3, Grad achieves slightly better results than GradInput. The poor performance of GNNEXPLAINER is probably caused by the dense feature masks, which do not separate the important features well.

5.5 Multiplicity of Explanations

We additionally find that multiple (disjoint) explanations of fidelity at least τ are indeed possible and frequent. We discuss the extension of ZORRO to retrieve multiple explanations in Appendix A. Figure 4 shows the number of nodes having multiple explanations. We observe that, without exception, all GNNs yield multiple disjoint explanations with $\approx 50\%$ of the 300 nodes under study have 2 to 10 explanations. Our algorithm’s disjoint explanations can be understood as a disjoint piece of evidence that would lead the model to the same decision. We expect a much larger number of overlapping explanations if the restrictive condition on disjointness is relaxed. However, the objective here is to show that a decision can be reached in multiple ways. Each explanation is a practical realization of a possible combination of nodes and features that constitutes a decision. We are the first to establish the multiplicity of explanations for GNN predictions.

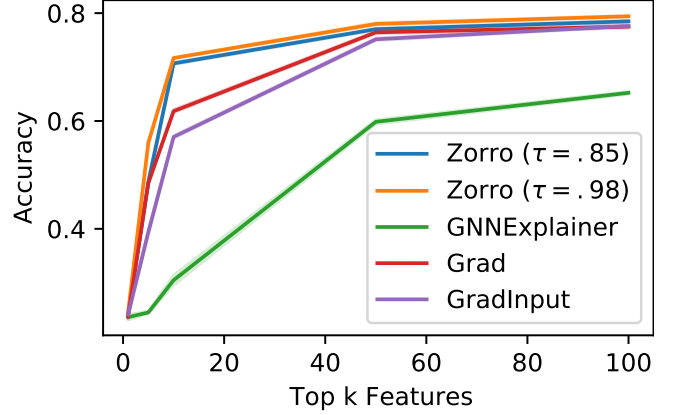


Figure 3: Test accuracy after retraining GCN on Cora based on the top k features. We repeated the retraining 20 times, report the mean, and observed a variation of below .001.

5.6 Insights into Model’s Behavior with Explanations

One of the motivations of post-hoc interpretability is to use explanations to derive insights into a model’s inner workings. GNNs are known to exploit the *homophily* in the neighborhood to learn powerful function approximators. We use the retrieved explanations by ZORRO to verify the models’ tendency to use homophily for node classification and identify the model’s mistakes. Formally, we define the homophily of the node as the fraction of the number of its neighbors, which share the same label as the node itself.

In what follows, we use homophily to refer to the homophily of a node with respect to the selected nodes in its first found explanation. True/Predicted homophily refers to the case when true/predicted node labels are used. We investigate the joint density of true and predicted homophily exhibited by the studied node sample. With an example plot of explanations on Cora dataset in 5, we illustrate the effect of connectivity and neighbors’ labels on model’s decision for a query node.

5.6.1 Influence of Nodes with Low Homophily. Nodes in the orange regions on the extreme left side of the plots are nodes that exhibited low true homophily but high predicted homophily. The class labels for such nodes are correctly predicted. However, the corresponding nodes in the explanation were assigned the wrong labels (if they were assigned the same labels as that of the particular node in question, its predicted homophily would have been increased). The density of such regions in APPNP is lower than in GCN, implying that APPNP makes fewer mistakes in assigning labels to neighbors of low homophily nodes. For example there are no nodes with true homophily 0 which influenced its neighbors in the incorrect way. These nodes can be further studied with respect to their degree and features.

5.6.2 Wrong Predictions Despite High Homophily. Several vertices corresponding to blue regions spread over the bottom of the plots have low predicted homophily. These nodes are incorrectly predicted, and their label differ from those predicted for the nodes in their explanation set. The surprising fact is that even though

Table 3: Analysis of the average sparsity, fidelity, and validity of the explanations. Here we compare the sparsity of the retrieved feature masks via effective explanation sizes as the input size is the same for all methods. The smaller the explanation size larger is the sparsity. As stability can be directly derived from fidelity and increases with fidelity > 0.5 (see Theorem 1), it suffices to compare fidelity to ensure stability.

Metric	Method	Cora				CiteSeer				PubMed			
		GCN	GAT	GIN	APNP	GCN	GAT	GIN	APNP	GCN	GAT	GIN	APNP
Sparsity	ZORRO ($\tau = .85$)	1.91	2.29	3.51	2.26	1.81	1.84	3.67	1.97	1.60	1.52	2.38	1.75
	ZORRO ($\tau = .98$)	2.69	3.07	4.34	3.18	2.58	2.60	4.68	2.78	2.55	2.58	3.21	2.86
	GNNEXPLAINER	7.27	7.27	7.27	7.27	8.21	8.21	8.21	8.21	6.21	6.21	6.21	6.21
	Grad	4.08	4.22	4.45	4.08	4.19	4.28	4.41	4.18	4.41	4.51	4.89	4.46
	GradInput	4.07	4.25	4.37	4.08	4.17	4.29	4.33	4.17	4.41	4.51	4.92	4.47
Fidelity	ZORRO ($\tau = .85$)	0.87	0.88	0.86	0.88	0.87	0.86	0.87	0.86	0.86	0.88	0.88	0.87
	ZORRO ($\tau = .98$)	0.97	0.97	0.96	0.97	0.97	0.97	0.97	0.96	0.96	0.97	0.97	0.96
	GNNEXPLAINER	0.71	0.66	0.52	0.65	0.68	0.69	0.51	0.62	0.67	0.73	0.67	0.72
	Grad	0.15	0.18	0.19	0.17	0.17	0.19	0.28	0.18	0.37	0.43	0.42	0.37
	GradInput	0.15	0.18	0.18	0.16	0.16	0.18	0.26	0.17	0.36	0.42	0.42	0.36
	Empty Explanation	0.15	0.18	0.18	0.16	0.16	0.18	0.26	0.17	0.36	0.42	0.42	0.36
Validity	ZORRO ($\tau = .85$)	1.00	1.00	0.83	1.00	1.00	1.00	0.77	1.00	0.90	1.00	0.84	1.00
	ZORRO ($\tau = .98$)	1.00	1.00	0.90	1.00	1.00	1.00	0.91	1.00	0.98	1.00	0.87	1.00
	GNNEXPLAINER	0.89	0.95	0.83	0.84	0.87	0.92	0.58	0.93	0.60	0.81	0.71	0.87
	Grad	0.26	0.25	0.15	0.18	0.28	0.25	0.12	0.26	0.36	0.49	0.50	0.38
	GradInput	0.22	0.22	0.12	0.17	0.18	0.16	0.08	0.19	0.36	0.49	0.50	0.37
	Empty Explanation	0.22	0.22	0.11	0.17	0.18	0.16	0.08	0.19	0.36	0.49	0.50	0.37

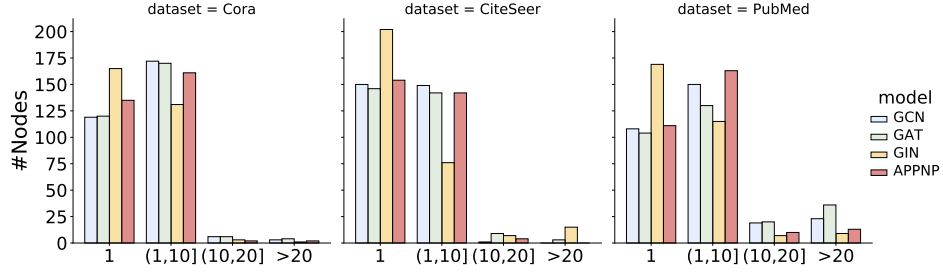


Figure 4: The number of explanations found with ZORRO at $\tau = 0.85$.

some of them have high true homophily close to 1, their predicted homophily is low. This also points to the usefulness of our found explanation in which we conclude that nodes influencing the current node do not share its label. So despite the general consensus of GNNs reliance on homophily, they can still do mistakes for high homophily nodes for example when information from features is misaligned (or leads to a different decision) with that from structure.

5.6.3 Incorrect High Homophily Predictions. We also note that for GIN and APPNP, we have some nodes with true homophily and predicted homophily close to 1 but are incorrectly predicted. This implies the node itself and the most influential nodes from its computational graph have been assigned the same label. We can conclude that the model based its decision on the right set of nodes but assigned the wrong class to the whole group.

6 RELATED WORK

Representation learning approaches on graphs encode graph structure with or without node features into low-dimensional vector

representations, using deep learning and nonlinear dimensional-reduction techniques. These representations are trained in an unsupervised [7, 12, 16] or semi-supervised manner by using neighborhood aggregation strategies and task-based objectives [14, 25].

Interpretability in Machine Learning. Post-hoc approaches to model interpretability are popularized by *feature attribution* methods that aim to assign importance to input features given a prediction either agnostic to the model parameters [19, 20] or using model specific attribution approaches [2, 24, 28]. *Instance-wise feature selection* (IFS) approaches [4, 5, 32], on the other hand, focuses on finding a *sufficient* feature subset or explanation that leads to little or no degradation of the prediction accuracy when other features are masked. The advantage of this formulation is that the output explanation has a precise meaning in terms of the predictive power of the chosen subset. Applying these works directly for graph models is infeasible due to the complex form of explanation, which should consider the complex association among nodes in addition to the input features.

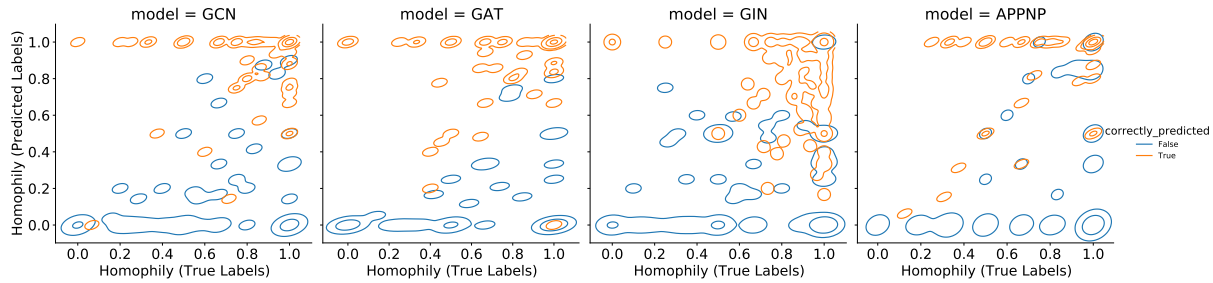


Figure 5: Dataset - PubMed. The joint distribution of the homophily with respect to the nodes selected in the ZORRO’s explanation ($\tau = .85$) with true and predicted labels. The orange contour lines correspond to the distributions for correctly predicted nodes, and the blue one corresponds to incorrectly predicted nodes.

Interpretability in GNNs. Model agnostic approaches like ours to interpretability in GNNs include GNNEXPLAINER [31], XGNN[33] and PGMEExplainer[26]. GNNEXPLAINER learns a real-valued graph mask and feature mask such that the mutual information with GNN’s predictions is maximized. XGNN proposed a reinforcement learning-based graph generation approach to generate explanations for the predicted class for a graph. We instead focus on explaining node level decisions. PGMEExplainer builds a simpler interpretable Bayesian network explaining the GNN prediction. Pope et al. [17] and Sanchez-Lengeling et al. [21] applied gradient based methods for explaining GNNs, which rely on propagating gradients/relevance from the output to the original model’s input features. Other works [9, 11] focus on explaining unsupervised network representations, which is out of scope for the current work.

7 CONCLUSION

We formulated the key properties a GNN explanation should follow: *validity*, *sparsity*, and *stability*. While none of these measures alone suffice to evaluate a GNN explanation, we introduce a new metric called *fidelity* that reflects these desiderata into a single measure. We provide theoretical foundations of fidelity from the area of *rate-distortion theory*. Furthermore, we proposed a simple combinatorial procedure ZORRO, which retrieves sparse *binary masks* for the features and relevant nodes while trying to optimize for fidelity. Our experimental results on synthetic and real-world datasets show massive improvements not only for fidelity but also concerning evaluation measures employed by previous works.

REFERENCES

- [1] Joris Baan, Maartje ter Hoeve, Marlies van der Wees, Anne Schuth, and Maarten de Rijke. 2019. Do Transformer Attention Heads Provide Transparency in Abstractive Summarization? *arXiv preprint arXiv:1907.00570* (2019).
- [2] Alexander Binder, Grégoire Montavon, Sebastian Lapuschkin, Klaus-Robert Müller, and Wojciech Samek. 2016. Layer-wise relevance propagation for neural networks with local renormalization layers. In *International Conference on Artificial Neural Networks*. Springer.
- [3] Oana-Maria Camburu, Eleonora Giunchiglia, Jakob Foerster, Thomas Lukasiewicz, and Phil Blunsom. 2020. The Struggles of Feature-Based Explanations: Shapley Values vs. Minimal Sufficient Subsets. *arXiv preprint arXiv:2009.11023* (2020).
- [4] Brandon Carter, Jonas Mueller, Siddhartha Jain, and David Gifford. 2018. What made you do this? understanding black-box decisions with sufficient input subsets. *arXiv preprint arXiv:1810.03805* (2018).
- [5] Jianbo Chen, Le Song, Martin J Wainwright, and Michael I Jordan. 2018. Learning to explain: An information-theoretic perspective on model interpretation. *arXiv preprint arXiv:1802.07814* (2018).
- [6] Matthias Fey and Jan E. Lenssen. 2019. Fast Graph Representation Learning with PyTorch Geometric. In *ICLR Workshop on Representation Learning on Graphs and Manifolds*.
- [7] Thorben Funke, Tian Guo, Alen Lancic, and Nino Antulov-Fantulin. 2020. Low-dimensional statistical manifold embedding of directed graphs. In *International Conference on Learning Representations*. <https://openreview.net/forum?id=SkxQp1StDH>
- [8] Sara Hooker, Dumitru Erhan, Pieter-Jan Kindermans, and Been Kim. 2019. A benchmark for interpretability methods in deep neural networks. In *Advances in Neural Information Processing Systems*. 9737–9748.
- [9] Maximilian Idahl, Megha Khosla, and Avishek Anand. 2019. Finding Interpretable Concept Spaces in Node Embeddings Using Knowledge Bases. In *Machine Learning and Knowledge Discovery in Databases - International Workshops of ECML PKDD 2019*. Springer, 229–240.
- [10] Alon Jacovi and Yoav Goldberg. 2020. Aligning Faithful Interpretations with their Social Attribution. *arXiv preprint arXiv:2006.01067* (2020).
- [11] Bo Kang, Jeffrey Lijffijt, and Tijl De Bie. 2019. Explaine: An approach for explaining network embedding-based link predictions. *arXiv preprint arXiv:1904.12694* (2019).
- [12] M. Khosla, V. Setty, and A. Anand. 2019. A Comparative Study for Unsupervised Network Representation Learning. *TKDE* (2019).
- [13] Pieter-Jan Kindermans, Sara Hooker, Julius Adebayo, Maximilian Alber, Kristof T Schütt, Sven Dähne, Dumitru Erhan, and Been Kim. 2019. The (un) reliability of saliency methods. In *Explainable AI: Interpreting, Explaining and Visualizing Deep Learning*. Springer, 267–280.
- [14] Thomas N. Kipf and Max Welling. 2017. Semi-Supervised Classification with Graph Convolutional Networks. In *ICLR*.
- [15] Johannes Klicpera, Aleksandar Bojchevski, and Stephan Günnemann. 2019. Predict then propagate: Graph neural networks meet personalized pagerank. *International Conference on Learning Representations (ICLR)* (2019).
- [16] Bryan Perozzi, Rami Al-Rfou, and Steven Skiena. 2014. Deepwalk: Online learning of social representations. In *KDD*. 701–710.
- [17] Phillip E Pope, Soheil Kolouri, Mohammad Rostami, et al. 2019. Explainability methods for graph convolutional neural networks. In *Proc. of the Conference on Computer Vision and Pattern Recognition*. 10772–10781.
- [18] Danish Pruthi, Mansi Gupta, Bhuwan Dhingra, Graham Neubig, and Zachary C Lipton. 2019. Learning to deceive with attention-based explanations. *arXiv preprint arXiv:1909.07913* (2019).
- [19] Marco Tulio Ribeiro, Sameer Singh, and Carlos Guestrin. 2016. "Why should i trust you?" Explaining the predictions of any classifier. In *Proceedings of the 22nd ACM SIGKDD international conference on knowledge discovery and data mining*. 1135–1144.
- [20] Marco Tulio Ribeiro, Sameer Singh, and Carlos Guestrin. 2018. Anchors: High-precision model-agnostic explanations. In *Thirty-Second AAAI Conference on Artificial Intelligence*.
- [21] Benjamin Sanchez-Lengeling, Jennifer Wei, Brian Lee, Emily Reif, Peter Wang, Wesley Wei Qian, Kevin McCloskey, Lucy Colwell, and Alexander Wiltchko. 2020. Evaluating Attribution for Graph Neural Networks. *Advances in Neural Information Processing Systems* 33 (2020).
- [22] Avanti Shrikumar, Peyton Greenside, and Anshul Kundaje. 2017. Learning important features through propagating activation differences. In *Proceedings of the 34th International Conference on Machine Learning-Volume 70*. JMLR. org, 3145–3153.

- [23] Chris R Sims. 2016. Rate–distortion theory and human perception. *Cognition* 152 (2016), 181–198.
- [24] Mukund Sundararajan, Ankur Taly, and Qiqi Yan. 2017. Axiomatic attribution for deep networks. In *Proceedings of the 34th International Conference on Machine Learning-Volume 70*. JMLR. org, 3319–3328.
- [25] Petar Veličković, Guillem Cucurull, Arantxa Casanova, Adriana Romero, Pietro Liò, and Yoshua Bengio. 2018. Graph Attention Networks. *ICLR* (2018).
- [26] Minh N. Vu and My T. Thai. 2020. PGM-Explainer: Probabilistic Graphical Model Explanations for Graph Neural Networks. In *Advances in Neural Information Processing Systems 33: Annual Conference on Neural Information Processing Systems 2020, NeurIPS 2020*.
- [27] Lior Wolf, Tomer Galanti, and Tamir Hazan. 2019. A formal approach to explainability. In *Proceedings of the 2019 AAAI/ACM Conference on AI, Ethics, and Society*, 255–261.
- [28] Kelvin Xu, Jimmy Ba, Ryan Kiros, Kyunghyun Cho, Aaron Courville, Ruslan Salakhutdinov, Rich Zemel, and Yoshua Bengio. 2015. Show, attend and tell: Neural image caption generation with visual attention. In *ICML*.
- [29] Keyulu Xu, Weihua Hu, Jure Leskovec, and Stefanie Jegelka. 2019. How Powerful are Graph Neural Networks?. In *International Conference on Learning Representations*.
- [30] Zhilin Yang, William W. Cohen, and Ruslan Salakhutdinov. 2016. Revisiting Semi-Supervised Learning with Graph Embeddings. *arXiv:1603.08861 [cs.LG]*
- [31] Rex Ying, Dylan Bourgeois, Jiaxuan You, Marinka Zitnik, and Jure Leskovec. 2019. GNN Explainer: A tool for post-hoc explanation of graph neural networks. *arXiv preprint arXiv:1903.03894* (2019).
- [32] Jinsung Yoon, James Jordon, and Mihaela van der Schaar. 2018. INVASE: Instance-wise variable selection using neural networks. (2018).
- [33] Hao Yuan, Jiliang Tang, Xia Hu, and Shuiwang Ji. 2020. XGNN: Towards Model-Level Explanations of Graph Neural Networks. In *KDD '20*. Association for Computing Machinery, 430–438.

APPENDIX

A DESIGN CHOICES FOR ZORRO

In the design of our ZORRO algorithm, we have made several choices, which we explicitly want to explain in detail here. In general, we have to make the following design choices: initialization of first element, iterative adding further elements, recursive design. Besides in Algorithm 4 we provide the generalization of ZORRO to extract multiple disjoint explanations of fidelity at least τ .

ZORRO - Variant for Retrieving Multiple Explanations

Algorithm 3 ZORRO(n, τ, K)

- 1: $V_n \leftarrow$ set of vertices in $G(n)$
 - 2: $F \leftarrow$ set of node features
 - 3: **return** ZORRO-Recursive(τ, K, V_n, F)
-

Algorithm 4 ZORRO-Recursive(τ, K, V_p, F_p)

- 1: $S = \emptyset, V_r = V_p, F_r = F_p, V_s = \emptyset, F_s = \emptyset$
 - 2: $V_r = V_p, F_r = F_p, V_s = \emptyset, F_s = \emptyset$
 - 3: $R_{V_p} \leftarrow$ list of $v \in V_p$ sorted by $\mathcal{F}(\{v\}, F_p)$
 - 4: $R_{F_p} \leftarrow$ list of $f \in F_p$ sorted by $\mathcal{F}(V_p, \{f\})$
 - 5: Add maximal element to V_s or F_s as in (7)
 - 6: **while** $\mathcal{F}(V_s, F_s) \geq \tau$ **do**
 - 7: $\tilde{V}_s = V_s \cup \operatorname{argmax}_{v \in \operatorname{top}_K(V_r)} \mathcal{F}(\{v\} \cup V_s, F_s)$
 - 8: $\tilde{F}_s = F_s \cup \operatorname{argmax}_{f \in \operatorname{top}_K(F_r)} \mathcal{F}(V_s, \{f\} \cup F_s)$
 - 9: **if** $\mathcal{F}(\tilde{V}_s, F_s) \leq \mathcal{F}(V_s, \tilde{F}_s)$ **then**
 - 10: $F_r = F_r \setminus \{f\}, F_s = \tilde{F}_s$
 - 11: **else**
 - 12: $V_r = V_r \setminus \{v\}, V_s = \tilde{V}_s$
 - 13: $S = S \cup \{V_s, F_s\}$
 - 14: $S = S \cup \text{ZORRO-Recursive}(\tau, K, V_p, F_p)$
 - 15: $S = S \cup \text{ZORRO-Recursive}(\tau, K, V_r, F_p)$
 - 16: **return** S
-

Initialization of first element. A single explanation $\{V_s, F_s\}$ consist of selected nodes V_s and selected features F_s . The challenge to select the first node and feature is the following: Selecting only a node or only a feature yields a non-informative value, i.e., $\mathcal{F}(\{v\}, \emptyset) = c$ and $\mathcal{F}(\emptyset, \{f\}) = c$ for all $v \in V_n$ and $f \in F$ and some constant $c \in [0, 1]$. The search for the optimal first pair would require $|V_p||F_p|$ evaluations of the fidelity, which is in most cases too expensive. Therefore, we propose to use a different strategy, which also contains information for the following iterations. Instead of evaluating, which pair of feature and node yields the highest increase, we assess the nodes and features in a maximal setting of the other. To be more precise, we assume that, if we search for the best node, all (possible) features F_p were unmasked:

$$\operatorname{argmax}_{v \in V_p} \mathcal{F}(\{v\}, F_p) \quad (8)$$

Similarly for the features, we assume that all (possible) nodes are unmasked:

$$\operatorname{argmax}_{f \in F_p} \mathcal{F}(V_p, \{f\}) \quad (9)$$

Whichever of the nodes or features yields the highest value is the first element of our explanation. Consequently, the next selected element is of a different type than the first element, e.g., if we first choose a node, the next element is always that feature, which yields the highest fidelity based on that single node. We perform this initialization again for each explanation since for each explanation, the maximal sets of possible elements V_p and F_p are different.

Iterative search. The next part of our algorithm, which is the main contributor to the computational complexity, is the iterative search for additional nodes and features after the first element. A full search of all remaining nodes and features would require $|V_r| + |F_r|$ fidelity computations. To significantly reduce this amount, we limited ourselves to a fixed number K nodes and features, see Algorithm 3. To systematically select the K elements, we use the information retrieved in the initialization by Eq. (8) and (9). We order the remaining nodes V_r and F_p by their values retrieved for Eq. (8) and (9) and only evaluate the top K . In Algorithm 3, we have denoted these orderings by R_{V_p} and R_{F_p} and the retrieval of the top K remaining elements by $\operatorname{top}_K(V_r, R_{V_p})$ and $\operatorname{top}_K(F_r, R_{F_p})$. We also experimented with evaluating all remaining elements but observed no performance gain or inferior performance to the above heuristic. As a reason, we could identify that in some cases, the addition of a single element (feature or node) could not increase the achieved fidelity. Using the ordering retrieved from the "maximal setting", we enforce that those elements are still selected, which contain valuable information with a higher likelihood. In addition, we experimented with refreshing the orderings R_{V_p} and R_{F_p} after some iterations but observed similar issues as in the unrestricted search.

Recursive design. We explicitly designed our algorithm in a way such that we can retrieve multiple explanations, see line 14 and line 15 of Algorithm 3. We recursively call the Algorithm 3 twice, once with a disjoint node-set, the call in line 15 (only elements from the remaining set of nodes V_r can be selected), and similarly in line 14 with a disjoint feature set. Hence, the resulting explanation selects disjoint elements from the feature matrix since either the rows or columns are different from before. As greedy and fast stop criteria, we used each further iteration, the maximal reachable fidelity of $\mathcal{F}(V_p, F_p)$.

Choice of Noisy Distribution \mathcal{N} . Our choice of using the global distribution of features as the noisy distribution ensures that only plausible feature values are used.

B PROOF OF THEOREM 2

PROOF. **Property 1** holds by construction of the algorithm. We start from an empty explanation and at any step (see lines 6 and 7 in Algorithm 1) the explanation subset is updated with a new feature or node only if the addition improves fidelity. The procedure stops only when an explanation of fidelity at least τ is retrieved.

For **Property 2** first, note that the while loop in Algorithm 1 (lines 7 till 13) runs for a maximum of $|V_n| + |F|$ iterations as in each step we either add a node or a feature to the explanation set. In practice, the number of iterations would be much smaller than the crude upper bound as we are able to find short explanations for most of the cases. For each iteration we compare the fidelity (line

10) of the explanation sets. A single computation of fidelity requires $O(\text{samples} \times t)$. The fidelity is computed using fixed number of samples (see Algorithm 2). Each iteration runs in time t which is the time required by one forward pass of the GNN. Combining all the above the run time complexity of ZORRO is given by $O(t \cdot \max(|V_n| + |F|))$.

Property 3 follows from the design of Algorithm 3. After retrieving an explanation, Algorithm 3 recursively call itself in line 14 and 15. In doing so, it checks for additional explanations with disjoint node and features. For additional reasoning see section A.

Property 4 follows from property 1 of ZORRO, Theorem 1 and observing the fact that $\tau(1 - \tau)$ decreases with respect to τ for $\tau \geq 0.5$. \square

C ADDITIONAL DETAILS FOR THE EXPERIMENTS

Datasets. Three well-known citation network datasets **Cora**, **CiteSeer** and **PubMed** from Yang et al. [30] where nodes represent documents and edges represent citation links. The class label is described by a similar word vector or an index of category. Statistics for these datasets can be found in Table 4. We used the datasets, including their training and test split from the PyTorch Geometric Library, which corresponds to the data published by Yang et al. [30].

Table 4: Datasets and statistics. The test accuracy is calculated on 1000 nodes.

Name	Class	d	$ V $	$ E $	Test Accuracy			
					GCN	GAT	GIN	APPNP
Cora	7	1433	2708	10556	0.794	0.791	0.679	0.799
CiteSeer	6	3703	3327	9104	0.675	0.673	0.480	0.663
PubMed	3	500	19717	88648	0.782	0.765	0.590	0.782

Hyperparameters. For ZORRO, we retrieved explanations for the threshold $\tau = 0.85$ and $\tau = 0.98$ and with $K = 10$. All fidelity values were calculated based on 100 samples. For all baselines we use the default hyperparameters. The GNN on the synthetic dataset we trained on 80% of the data and used Adam optimizer with learning rate 0.001, and weight decay 0.005 for 2000 epochs. On the real datasets, we use the default training split of 10 samples per class and applied Adam optimizer with learning rate 0.01, and weight decay 0.005 for 200 epochs. We refer to the available implementation, for further details of the models and the training of the GNNs. We also include the saves of the trained model to increase the reproducibility. Our implementation is based on PyTorch Geometric 1.6 [6] and Python 3.7. All methods were executed on a server with 128 GB RAM and Nvidia GTX 1080Ti.

Experiments on synthetic dataset. The synthetic dataset is generated by generating two communities consisting of house motifs attached to BA graphs. Each node has eight feature values drawn from $\mathcal{N}(0, 1)$ and two features drawn from $\mathcal{N}(-1, .5)$ for nodes of the first community or $\mathcal{N}(1, .5)$ otherwise. In addition, to follow the published implementation of GNNExplainer, the feature values are

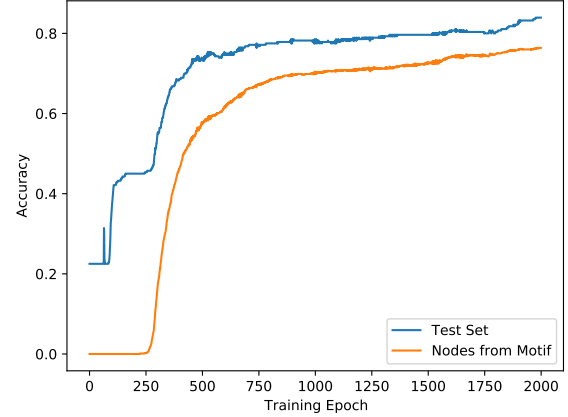


Figure 6: Accuracy of the GCN trained on synthetic dataset. We recorded the accuracy for the test set and the nodes in the motif, which are explained in the experiments.

Table 5: Accuracy of the selected epochs for the test set and the nodes in the motif.

Epoch	Test Accuracy	Motif Accuracy
0	0.22	0.00
200	0.45	0.00
400	0.69	0.47
600	0.75	0.62
1400	0.80	0.72
2000	0.84	0.76

normalized within each community, and within each community, 0.01 % of the edges are randomly perturbed.

The eight labels are given by the following: for each community, the nodes of the BA graph form a class, the 'basis' of the house forms a class, the 'upper' nodes form a class, and the rooftop is a class. The used model is a three-layer GCN, which stacks each layer's latent representation and uses a linear layer to make the final prediction. The training set includes 80% of the nodes.

Since GNNExplainer only returns soft edge mask, we sorted them and added both nodes from the highest-ranked edges until at least five nodes were selected. In this way, we retrieved hard node masks, which are necessary to compare with the ground truth.

Performance of model at different training epochs. Figure 6 illustrates the performance during the epochs and Table 5 states the details of the selected epochs.